Quantum-to-Classical Transition of Proton Transfer in Potential-Induced Dioxygen Reduction

Ken Sakaushi,[1,2,*] Andrey Lyalin,[2] Tetsuya Taketsugu,[2,3,4] and Kohei Uosaki[1,2]
[1]Center for Green Research on Energy and Environmental Science, National Institute for Materials Science, Namiki 1-1, Tsukuba 305-0044, Japan
[2]Global Research Center for Environment and Energy based on Nanomaterials Science, National Institute for Materials Science, Namiki 1-1, Tsukuba 305-0044, Japan
[3]Department of Chemistry, Faculty of Science, Hokkaido University, Sapporo 060-0810, Japan
[4]Institute for Chemical Reaction Design and Discovery (WPI-ICReDD), Hokkaido University, Sapporo 001-0021, Japan

(Received 31 August 2018; revised manuscript received 22 October 2018; published 7 December 2018)

We report an observation of a quantum tunneling effect in a proton-transfer (PT) during potential-induced transformation of dioxygen on a platinum electrode in a low overpotential (η) region at 298 K. However, this quantum process is converted to the classical PT scheme in the high η region. Therefore, there is a quantum-to-classical transition of the PT (QCT-PT) process as a function of the potential, which is confirmed by theoretical analysis. This observation indicates that the quantum tunneling governs the multistep electron-proton-driven transformation of dioxygen in the low η condition.

DOI: 10.1103/PhysRevLett.121.236001

Quantum tunneling plays vital roles in a wide spectrum of physical, chemical, and biological processes, providing efficient functions to life and modern technology [1–7]. The basic principle of quantum tunneling is the transmission of particles through an activation barrier due to its nonzero permeability [1,8], instead of overcoming the barrier via the transition state [9]. Especially, quantum proton tunneling can emerge as various significant effects in key physical phenomena in a wide range of temperature [10–13]. Usually in physical or chemical processes the activation barrier is predefined by a combination of the reactant and product of the reaction. Therefore, once the initial and final states of the process are fixed and the activation barrier is known, one can calculate the permeability of the barrier for each elementary step of the process and predict the probability of the quantum tunneling [14]. On the other hand, in the case of potential-induced processes, for instance, multielectron–multiproton transfer in electrochemical reactions [15,16], one can alter the energy of the initial or final state by applying the external potential. That means that the height of an activation barrier can be a function of the potential via the simple Brønsted-Evans-Polanyi relationship [17,18], and hence one can expect unique phenomena when the ratio of probabilities to overcome the barrier classically via the transition state and quantumly via tunneling through the barrier can be modified by the potential. In other words, one can switch on or off quantum-mechanical tunneling by changing the height of the barrier. In spite of the simplicity of this idea such a phenomenon has not been observed to the best of our knowledge.

In this Letter, we demonstrate observation of the quantum-to-classical transition of proton transfer (QCT-PT) in the process of potential-induced dioxygen reduction on a platinum electrode at 298 K. Our results clearly show the appearance of the QCT-PT in the electrode process as a function of the potential: at lower overpotential conditions (high barrier, when overcoming via transition state becomes difficult), the proton prefers to be transferred by quantum tunneling, while at high overpotentials (small barrier, when overcoming the barrier via transition state becomes favorable) the classical mechanism of overcoming the activation

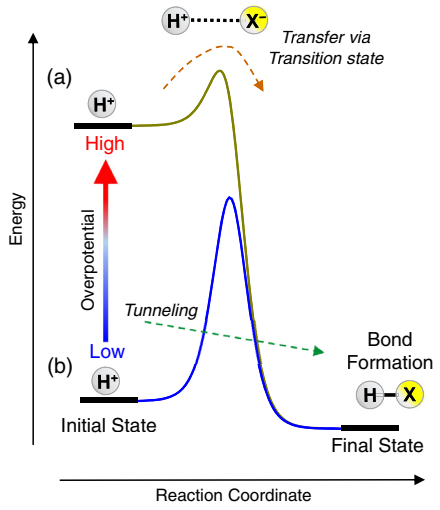

FIG. 1. Schematic diagram for two possible paths of the proton-transfer reaction: (a) proton transfer via the transition state (classical); (b) proton tunneling through the barrier (quantum). In the electrochemical system the relative contribution of the two mechanisms can be tuned by the applied potential.

barrier controls the process, as schematically illustrated in Fig. 1.

We show that QCT-PT can be observed in the potential-induced O_2 reduction process on the Pt electrode in alkaline solution, when four hydroxide ions are produced by transferring four electrons and four protons supplied from two water molecules into dioxygen: $O_2 + 2H_2O + 4e^- \rightarrow 4OH^-$. As a descriptor of quantum tunneling in PT and the quantum-to-classical transition effect we have investigated the hydrogen or deuterium kinetic isotopic rate constant ratio $k_H/k_D(\equiv K^{H/D})$. By measuring $K^{H/D}$, we can clarify the nature of the PT processes because the replacement of hydrogen by deuterium can considerably affect the reaction rates of electrode processes [19–22]. We show that $K^{H/D} = 32$ for O_2 reduction on Pt in alkaline conditions and this value drops down to 3.7 as a function of the potential. The large value of $K^{H/D} = 32$ considerably exceeds this semiclassical limit indicating manifestation of the tunneling effect [19]. Therefore, our results clearly demonstrate the appearance of the quantum-to-classical transition in the electrode process as a function of potential, as schematically illustrated in Fig. 1. Thus, it is demonstrated that proton tunneling can play an important role in the microscopic electrode processes of O_2 reduction when a number of conditions are fulfilled and shows exciting undiscovered insights of a key electrochemical process.

Since the overpotential-dependent $K^{H/D}$ is defined as the ratio of the isotopic rate constants, one can obtain this value from the following general equations:

$$K^{H/D} = \frac{k_0^H}{k_0^D} = \frac{j_0^H}{j_0^D}\frac{C_0^D}{C_0^H}\exp\left(\frac{(\alpha^D - \alpha^H)F\eta}{RT}\right), \quad (1)$$

$$j = j_0 \exp\left(-\frac{\alpha F\eta}{RT}\right), \quad (2)$$

$$j_0 = nFk_0C_0, \quad (3)$$

where j_0, C_0, α, η, F, R, and T are exchange current density, oxygen concentration, transfer coefficient, overpotential, Faraday constant, gas constant, and temperature (298 ± 1 K in this experiment), respectively. The superscripts H and D indicate the values in H_2O and D_2O systems, respectively. For the calculation of the pD in alkaline conditions, we remind that the dissociation constant of D_2O is different from that of H_2O [22]. Furthermore, in order to avoid unknown liquid junction effects due to the use of reference electrodes such as an Ag/AgCl electrode [23,24], we used reversible hydrogen or deuterium electrodes by following the protocol of Yeager and his co-workers [25]. Prior to discussing the dioxygen reduction process, the cyclic voltammogram and linear-sweep voltammetry combined with rotating ring-disk electrode technique were applied to check that the experimental H_2O and D_2O systems work properly

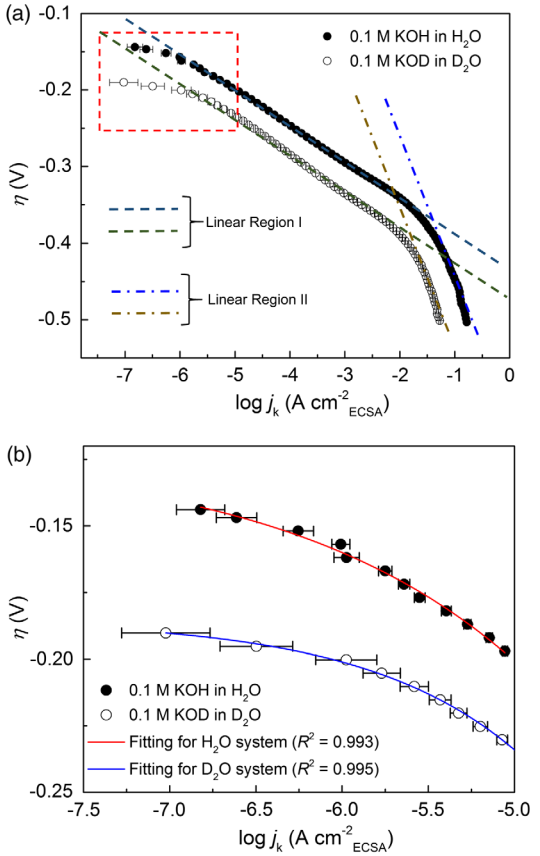

FIG. 2. Overpotential vs log j_k diagram of Pt in O_2-saturated 0.1 M KOD and 0.1 M KOH solutions. (a) Three different regions to obtain Tafel slope: low overpotential region (area surrounded by red dotted line), linear region I (middle overpotential), and linear region II (high overpotential). (b) Enlarged overpotential vs log j_k diagram in the low overpotential region, $-0.2\ \text{V} < \eta < -0.1\ \text{V}$. A detailed method for the fitting of plots is described in the Supplemental Material [26]. The coefficient of determination, R^2, for H_2O and D_2O systems is 0.993 and 0.995, respectively.

(Supplemental Material [26], Fig. S1). We used $n = 4$ for both H_2O and D_2O systems based on the experimental results (Supplemental Material [26], Fig. S2). All observed currents were normalized by electrochemical active surface area (ECSA). The C_0^D/C_0^H is known to be 1.101. The equilibrium potential for D_2O formation, $E^0_{D_2O}$, can be calculated by thermophysical values (see, e.g., Ref. [25] and references therein) and we obtain $E^0_{D_2O} = 1.262$ V vs reversible deuterium electrode. The transfer coefficient α can be obtained from the Tafel slope, b:

$$\alpha = \frac{2.303RT}{Fb}. \quad (4)$$

The O_2 reduction kinetics in 0.1 M KOH in H_2O and 0.1 M KOD in D_2O were analyzed by comparing the kinetic currents presented in Fig. 2 and Table I. A detailed method to obtain kinetic values is well described in our previous report [22]. Since Pt is known to show clear

TABLE I. Summary of O_2 reduction kinetics and $K^{H/D}$.

Region	Tafel slope (V/dec)	α	$-\log j_0^H$ (A/cm^2_{ECSA})	$-\log j_0^D$ (A/cm^2_{ECSA})	$K^{H/D}$
Low η	0.031 ± 0.003	1.91 ± 0.17	11 ± 0	12 ± 1	32 ± 4
Middle η	0.047 ± 0.002	1.26 ± 0.05	9.1 ± 0.1	9.8 ± 0.0	5.5 ± 0.2
High η	0.22 ± 0.01	0.27 ± 0.01	3.0 ± 0.0	3.6 ± 0.2	3.7 ± 0.2

diffusion limiting current j_{lim}, the O_2 reduction kinetic currents can be separated from diffusion limiting current by using the simple following equation:

$$\frac{1}{j} = \frac{1}{j_k} + \frac{1}{j_{lim}} \Leftrightarrow j_k = \frac{j_{lim} \cdot j}{j_{lim} - j}. \quad (5)$$

The value of the Tafel slope b was confirmed to be around 0.05 V/dec in the linear region I (middle η region, -0.35 V $< \eta < -0.2$ V) and shifted to 0.2 V/dec at the linear region II (high η region, -0.5 V $< \eta < -0.4$ V); see Fig. 2(a) for details. These regions are selected by following the procedure reported in Ref. [27]. In the lower overpotential region, -0.2 V $< \eta < -0.1$ V, there is no linear dependence of η on $\log j_k$, as is seen from Fig. 2(b); therefore the Tafel slope $b = 0.03$ V/dec was taken as a representative value to calculate $K^{H/D}$ in the low overpotential region, as shown in Table I [28]. For the detailed analysis, the plots in the low overpotential region [Fig. 2(b)] were fitted to obtain the Tafel relation (see Supplemental Material [26]), and this relation was used to calculate $K^{H/D}$. From this fact, as shown above, α was obtained in different overpotentials and the overpotential dependence of $K^{H/D}$ was checked by using these values.

As the results from Eqs. (1)–(4) and Table I, $K^{H/D}$ of Pt in three different regions (low, middle, and high overpotential regions) can be obtained as 32 ± 4, 5.5 ± 0.2, and 3.7 ± 0.2, respectively. Our results indicate that the rate-determining step of O_2 reduction in the alkaline condition contains proton transfer. An anomalously large value of $K^{H/D} > 13$ in the low overpotential region indicates manifestation of the quantum-proton tunneling, which is a classically forbidden proton-transfer mechanism. This is because the maximum KIE for the O-H bond breaking is ~13 at 298 K based on the semiclassical theory accounting for the change in the reaction barrier due to the differences in zero-point energies associated with the stretching and bending vibrations in O-H and O-D (see, e.g., Ref. [19] and references therein). Furthermore, it is known that the adsorption energies of OH and OD on the Pt surface can be different due to the differences in zero-point energies [29]. In addition to this, it has been suggested that the oxygen reduction reaction (ORR) rate on Pt is governed by OH adsorption [30]. However, we found that the difference in OH/OD adsorption energies in our system is 1.2 kJ/mol, which is similar to values reported in Ref. [29], and this difference should not affect our conclusion (see Supplemental Material [26], Figs. S4 and S5 for the detailed discussion. In order to obtain the OH/OD adsorption energies we have followed the method described in Ref. [31]). By combining previous reports [32,33], and our experimental observations [22], it can be concluded that the proton-transfer process is related to the rate-determining step of O_2 reduction in alkaline conditions. Furthermore, we have demonstrated manifestation of the quantum tunneling process for the proton transfer in the low overpotential region, which is vanishing in the high overpotentials, showing quantum-to-classical transition, i.e., QCT-PT.

In order to understand the observed phenomenon we carried out a theoretical analysis of the KIE in the proton transfer accounting for the probability of tunneling in O_2 reduction. Recent theoretical work has clearly

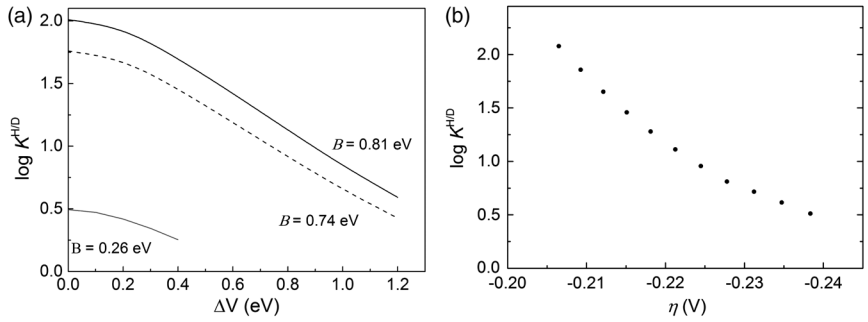

FIG. 3. (a) Dependence of $\log K^{H/D}$ on the reaction exothermicity ΔV, calculated for the values of the proton transfer barrier at equilibrium $B = 0.26$ [41], 0.74 [43], and 0.81 eV [44] reported in the literature. (b) Experimentally obtained $\log K^{H/D}$ vs η plots in a low overpotential region.

demonstrated that the O_2 reduction on Pt in the alkaline solution mainly occurs via the $(H_2O)_{ads}$-mediated mechanism, where protons transfer from the water molecules adsorbed on the surface in an organized network structure in a series of reactions [34]:

$$(O_2)_{sol} + * \rightarrow (O_2)_{ads}, \tag{6a}$$

$$(O_2)_{ads} + (H_2O)_{ads} \rightarrow (OOH)_{ads} + (OH)_{ads}, \tag{6b}$$

$$(O)_{ads} + (H_2O)_{ads} \rightarrow 2(OH)_{ads}, \tag{6c}$$

$$(OOH)_{ads} \rightarrow (O)_{ads} + (OH)_{ads}, \tag{6d}$$

$$(OH)_{ads} + e^- \rightarrow * + (OH)^-_{sol}, \tag{6e}$$

where the asterisk denotes the surface, while subscript indices ads and sol correspond to the adsorbed and solution species, respectively. In the first step (6a) dioxygen is adsorbed on the Pt surface, followed by the proton transfer from the adsorbed $(H_2O)_{ads}$ to $(O_2)_{ads}$ and $(O)_{ads}$ intermediates as well as $(OOH)_{ads}$ dissociation in steps (6b), (6c), and (6d), respectively. In the final step (6e), $(OH)_{ads}$ dissolves to $(OH)_{ads}$ as a result of the one electron reduction. The above mechanism proposed by Liu *et al.* [34] is different from the well-known associative and dissociative mechanisms of reduction by $(H_2O)_{sol}$, typically considered for the ORR in acid solution [30]. It should be noted that the steps (6b)–(6d) involve no electron transfer, and therefore are potentially independent; however, the adsorption energy of ORR intermediates depends on the $(OH)_{ads}$ coverage, which is the potential dependent. Further details can be found in Ref. [34]. The $(H_2O)_{ads}$-mediated mechanism of the dioxygen reduction leads to the formation of $(OOH)_{ads}$, $(O)_{ads}$, and $(OH)_{ads}$ intermediates. Such processes consist of bond breaking or formation with proton, which is O-H bond breaking of H_2O and then formation of an O-H bond with one of the intermediates. Based on the above considerations, we analyzed our experimental results by using a theoretical approach.

A simple estimation of the reaction rate constants accounting for the tunneling probability of the proton through the potential barrier can be performed by approximating the barrier by the asymmetric Eckart's one-dimensional potential energy function of the barrier height V_1, reaction exothermicity parameter ΔV, and the width a (see Supplemental Material [26], for details) [19,35,36]. Such a simple but robust approach gives a clear physical picture of the process and has been successfully used in a number of tunneling model analyses of experimental data [37], and is able to accurately reproduce the experimentally obtained reaction rates and isotopic rate constant ratios in a large range of temperatures except low ($T < 50$ K) temperatures where it is necessary to take into account zero point energy effects [36]. Note that a more consistent description of the tunneling process should take into account reorganization of the many degrees of freedom [38–40].

In the case of the potential-induced process, parameters of the barrier height and exothermicity can be altered via applied potentials. In the present work the Brønsted-Evans-Polanyi (BEP) relationship was used to describe linear variations in the barrier height with the reaction energy,

$$V_1 = -A\Delta V + B, \tag{7}$$

where A characterizes the position of the transition state along the reaction coordinate, herein taken to be 0.5, and B is the barrier height at the equilibrium, i.e., when $\Delta V = 0$ [41]. Alternatively, a more realistic form of the potential barrier for the proton transfer at the electrode-water interface can be evaluated by first-principles atomic-scale simulations under bias potential [42].

Using the Eckart barrier with the height defined by the BEP relationship we have calculated the $K^{H/D}$ for the proton transfer from the water molecule adsorbed on the surface to the possible intermediates of O_2 reduction reported by Liu *et al.* [34], with the use of the computer code described by Le Roy [35]. It should be noted that the tunneling probability is strongly affected by the barrier width as shown in Fig. S3 in the Supplemental Material [26]. We estimated the barrier width parameter a to be equal to 0.3 Å using theoretical data on the optimized structures for the adsorption of the reaction intermediates covered by a bilayer of water on Pt surface [34]. The consistent theoretical analysis of the tunneling effect in electrocatalytic oxygen reduction would require direct calculation of the energy barrier profile for proton transfer which goes far beyond the scope of the present work. It has been shown that in the optimized configuration the length of the hydrogen bond between the chemisorbed water molecule and $(O)_{ads}$ intermediate is 1.96 Å [34], which should correspond to the linear reaction path length of 0.99 Å, as the length of the O-H bond in the reaction product is 0.97 Å. In the case of the $(O_2)_{ads}$ intermediate two hydrogen bonds with water bilayer are formed with the bond length of 1.74 and 1.90 Å, which would correspond to the linear reaction path length for proton transfer of 0.77 and 0.93 Å, respectively. For the $(OH)_{ads}$ intermediate the hydrogen bond between $(OH)_{ads}$ and $(H_2O)_{ads}$ is 1.62 Å. These reaction path lengths correspond to the values of the barrier width lying in the range of $a = 0.25$–0.35 Å. Therefore, we selected $a = 0.3$ Å as a typical value for the width of the Eckart's barrier used in this study and also investigated how KIE depends on the barrier width a (see Fig. S3 of the Supplemental Material [26]).

The value of the barrier height B for the proton transfer for the steps at the equilibrium is open to debate, and the reported values vary from 0.26 to 0.81 eV [41,43,44]. Therefore, we have calculated the dependence of $\log K^{H/D}$ on exothermicity ΔV for several available values of the

proton transfer barrier at equilibrium; see Fig. 3(a). Results of our theoretical analysis demonstrate that for the small values of ΔV, the tunneling effect dominates in the proton transfer in a good agreement with the experimental observation of the $\log K^{\mathrm{H/D}} - \eta$ relation in the low overpotential region; see Fig. 3(b). For further details of mathematical models and procedures, see the Supplemental Material [26]. It is interesting that for $B = 0.74$ eV reported by Sugino *et al*. [43], and for $B = 0.81$ eV reported by Janik *et al*. [44], the maximum $\log K^{\mathrm{H/D}}$ is equal to 1.76 and 2.01, respectively, which are very close to the experimentally observed value of $\log K^{\mathrm{H/D}} = 2.1$ at $\eta = -0.208$, where the $K^{\mathrm{H/D}}$ value was obtained at the minimum overpotential to be observable in our experiment; therefore, probably this $K^{\mathrm{H/D}}$ value is close to the maximum and can be the limit to be verified by our mathematical models. Nevertheless, both the theoretical and experimental results demonstrate that tunneling can be observed in the low overpotential regime while the proton transfer process becomes classical at higher overpotentials. Our combined theoretical and experimental study clearly demonstrates the manifestation of the potential-dependent KIE in electrochemical systems. The observed QCT-PT phenomenon in the proton-transfer mechanism as a function of potential shows that the tunneling can dominate in the proton transfer in the low η region because in this case it has higher probability than overcoming the activation barrier classically via transition state. However, in the higher η region, the barrier becomes low enough and therefore the classical proton-transfer mechanism controls the overall process.

In conclusion, we have shown that there is a quantum-to-classical transition in potential-induced oxygen reduction on the platinum electrode in alkaline solution where proton tunneling can play an important role in the low overpotential regime. Likewise, unexpected strong effects of adsorbed ions or crystal structures can alter the kinetics of electrochemical reactions [32]; this study indicates the nontrivial importance of proton transfer in the microscopic electrode process of dioxygen reduction and can affect its kinetics. We believe that understanding of the quantum proton-transfer mechanism described in the present work is key to clarify the fundamental physical principles in complicated electrode processes. The quantum tunneling effect and the analytical approach based on KIE shown here can be an additional powerful tool to obtain new insights to this process. These could help to build more accurate theoretical models and combine them to experimental systems in order to unveil the complicated multielectron-multiproton transfer reactions at electrodes.

K. S. is indebted to National Institute for Materials Science, Japan Prize Foundation Research Grant, and Program for Development of Environmental Technology using Nanotechnology of MEXT for supports. This work was partially supported by JSPS KAKENHI Grants No. 17K14546 and No. 15K05387. K. S. and A. L. deeply thank Professor Robert J. Le Roy (Waterloo University, Canada) for providing us his original code described in Ref. [35].

*Corresponding author.
sakaushi.ken@nims.go.jp

[1] F. Hund, Zur Deutung der Molekelspektren. III, Z. Phys. **43**, 805 (1927).
[2] L. Esaki, New phenomenon in narrow germanium $p - n$ junctions, Phys. Rev. **109**, 603 (1958).
[3] G. Binnig, H. Rohrer, C. Gerber, and E. Weibel, Tunneling through a controllable vacuum gap, Appl. Phys. Lett. **40**, 178 (1982).
[4] Y. Cha, C. J. Murray, and J. P. Klinman, Hydrogen tunneling in enzyme reactions, Science **243**, 1325 (1989).
[5] P. R. Schreiner, H. P. Reisenauer, D. Ley, D. Gerbig, C.-H. Wu, and W. D. Allen, Methylhydroxycarbene: Tunneling control of a chemical reaction, Science **332**, 1300 (2011).
[6] L. Britnell, R. V. Gorbachev, R. Jalil, B. D. Belle, F. Schedin, A. Mishchenko, T. Georgiou, M. I. Katsnelson, L. Eaves, S. V. Morozov, N. M. R. Peres, J. Leist, A. K. Geim, K. S. Novoselov, and L. A. Ponomarenko, Field-effect tunneling transistor based on vertical graphene heterostructures, Science **335**, 947 (2012).
[7] Q. H. Wang, K. Kalantar-Zadeh, A. Kis, J. N. Coleman, and M. S. Strano, Electronics and optoelectronics of two-dimensional transition metal dichalcogenides, Nat. Nanotechnol. **7**, 699 (2012).
[8] R. P. Bell, The tunnel effect correction for parabolic potential barriers, Trans. Faraday Soc. **55**, 1 (1959).
[9] P. Hänggi, P. Talkner, and M. Borkovec, Reaction-rate theory: Fifty years after Kramers, Rev. Mod. Phys. **62**, 251 (1990).
[10] M. E. Tuckerman and D. Marx, Heavy-Atom Skeleton Quantization and Proton Tunneling in "Intermediate-Barrier" Hydrogen Bonds, Phys. Rev. Lett. **86**, 4946 (2001).
[11] S. Horiuchi, Y. Tokunaga, G. Giovannetti, S. Picozzi, H. Itoh, R. Shimano, R. Kumai, and Y. Tokura, Above-room-temperature ferroelectricity in a single-component molecular crystal, Nature (London) **463**, 789 (2010).
[12] C. Drechsel-Grau and D. Marx, Quantum Simulation of Collective Proton Tunneling in Hexagonal Ice Crystals, Phys. Rev. Lett. **112**, 148302 (2014).
[13] X. Meng, J. Guo, J. Peng, J. Chen, Z. Wang, J.-R. Shi, X.-Z. Li, E.-G. Wang, and Y. Jiang, Direct visualization of concerted proton tunnelling in a water nanocluster, Nat. Phys. **11**, 235 (2015).
[14] D. G. Truhlar, B. C. Garrett, and S. J. Klippenstein, Current status of transition-state theory, J. Phys. Chem. **100**, 12771 (1996).
[15] R. W. Gurney, The quantum mechanics of electrolysis, Proc. R. Soc. A **134**, 137 (1931).
[16] S. G. Christov, Die Rolle des Tunnelübergangs der Ionen in der Kinetik der Elektrodenvorgänge, Z. Elektrochem. **62**, 567 (1958).
[17] J. N. Bronsted, Acid and basic catalysis, Chem. Rev. **5**, 231 (1928).

[18] M. G. Evans and M. Polanyi, Inertia and driving force of chemical reactions, Trans. Faraday Soc. **34**, 11 (1938).
[19] R. P. Bell, *The Tunnel Effect in Chemistry* (Chapman and Hall, London, 1980).
[20] J. Horiuti, K. Hirota, and G. Okamoto, Application of transition state method to the heterogeneous reaction on hydrogen electrode, Sci. Papers Inst. Phys. Chem. Res. **29**, 223 (1936).
[21] B. E. Conway, Kinetics of electrolytic hydrogen and deuterium evolution, Proc. R. Soc. A **256**, 128 (1960).
[22] K. Sakaushi, M. Eckardt, A. Lyalin, T. Taketsugu, R. J. Behm, and K. Uosaki, Microscopic electrode processes in the four-electron oxygen reduction on highly active carbon-based electrocatalysts, ACS Catal. **8**, 8162 (2018).
[23] E. C. M. Tse, J. A. Varnell, T. T. H. Hoang, and A. A. Gewirth, Elucidating proton involvement in the rate-determining step for pt/pd-based and non-precious-metal oxygen reduction reaction catalysts using the kinetic isotope effect, J. Phys. Chem. Lett. **7**, 3542 (2016).
[24] D. Malko and A. Kucernak, Kinetic isotope effect in the oxygen reduction reaction (ORR) over Fe-N/C catalysts under acidic and alkaline conditions, Electrochem. Comm. **83**, 67 (2017).
[25] M. M. Ghoneim, S. Clouser, and E. Yeager, Oxygen reduction kinetics in deuterated phosphoric acid, J. Electrochem. Soc. **132**, 1160 (1985).
[26] See Supplemental Material at http://link.aps.org/supplemental/10.1103/PhysRevLett.121.236001 for experimental procedures, and additional experimental/theoretical data and related discussions.
[27] J. X. Wang, N. M. Markovic, and R. R. Adzic, Kinetic analysis of oxygen reduction on Pt(111) in acid solutions: Intrinsic kinetic parameters and anion adsorption effects, J. Phys. Chem. B **108**, 4127 (2004).
[28] S. Fletcher, Tafel slopes from first principles, J. Solid State Electrochem. **13**, 537 (2009).
[29] E. M. Karp, C. T. Campbell, F. Studt, F. Abild-Pedersen, and J. K. Nørskov, Energetics of oxygen adatoms, hydroxyl species and water dissociation on Pt(111), J. Phys. Chem. C **116**, 25772 (2012).
[30] J. K. Nørskov, J. Rossmeisl, A. Logadottir, L. Lindqvist, J. R. Kitchin, T. Bligaard, and H. Jónsson, Origin of the overpotential for oxygen reduction at a fuel-cell cathode, J. Phys. Chem. B **108**, 17886 (2004).
[31] F. Calle-Vallejo, J. Tymoczko, V. Colic, Q. H. Vu, M. D. Pohl, K. Morgenstern, D. Loffreda, P. Sautet, W. Schuhmann, and A. S. Bandarenka, Finding optimal surface sites on heterogeneous catalysts by counting nearest neighbors, Science **350**, 185 (2015).
[32] N. M. Marković and P. N. Ross, Surface science studies of model fuel cell electrocatalysts, Surf. Sci. Rep. **45**, 117 (2002).
[33] M. R. Tarasevich, A. Sadkowski, and E. Yeager, Oxygen electrochemistry, in *Comprehensive Treatise of Electrochemistry: Volume 7 Kinetics and Mechanisms of Electrode Processes*, edited by B. E. Conway, J. O. Bockris, E. Yeager, S. U. M. Khan, and R. E. White (Springer, Boston, MA, 1983), pp. 301–398.
[34] S. Liu, M. G. White, and P. Liu, Mechanism of oxygen reduction reaction on Pt(111) in alkaline solution: Importance of chemisorbed water on surface, J. Phys. Chem. C **120**, 15288 (2016).
[35] R. J. Le Roy, H. Murai, and F. Williams, Tunneling model for hydrogen abstraction reactions in low-temperature solids. Application to reactions in alcohol glasses and acetonitrile crystals, J. Am. Chem. Soc. **102**, 2325 (1980).
[36] R. J. Le Roy, E. D. Sprague, and F. Williams, Quantum mechanical tunneling in hydrogen atom abstraction for solid acetonitrile at 77 − 87°K, J. Phys. Chem. **76**, 546 (1972).
[37] G. Brunton, D. Griller, L. R. C. Barclay, and K. U. Ingold, Kinetic applications of electron paramagnetic resonance spectroscopy. 26. Quantum-mechanical tunneling in the isomerization of sterically hindered aryl radicals, J. Am. Chem. Soc. **98**, 6803 (1976).
[38] M. Tachikawa, K. Mori, H. Nakai, and K. Iguchi, An extension of ab initio molecular orbital theory to nuclear motion, Chem. Phys. Lett. **290**, 437 (1998).
[39] J. Grimminger, S. Bartenschlager, and W. Schmickler, A model for combined electron and proton transfer in electrochemical systems, Chem. Phys. Lett. **416**, 316 (2005).
[40] S. Hammes-Schiffer, Proton-coupled electron transfer: Moving together and charging forward, J. Am. Chem. Soc. **137**, 8860 (2015).
[41] V. Tripković, E. Skúlason, S. Siahrostami, J. K. Nørskov, and J. Rossmeisl, The oxygen reduction reaction mechanism on Pt(111) from density functional theory calculations, Electrochim. Acta **55**, 7975 (2010).
[42] A. Bouzid and A. Pasquarello, Atomic-scale simulation of electrochemical processes at electrode/water interfaces under referenced bias potential, J. Phys. Chem. Lett. **9**, 1880 (2018).
[43] N. Bonnet, M. Otani, and O. Sugino, Self-poisoning dynamical effects in the oxygen reduction reaction on Pt (111) from a top-down kinetic analysis, J. Phys. Chem. C **118**, 13638 (2014).
[44] M. J. Janik, C. D. Taylor, and M. Neurock, First-principles analysis of the initial electroreduction steps of oxygen over Pt(111), J. Electrochem. Soc. **156**, B126 (2009).